Physical Adsorption of Charged Plastic Nanoparticles Affects Algal Photosynthesis

ARTICLE · JANUARY 2010

CITATIONS
28

READS
252

4 AUTHORS, INCLUDING:

Priyanka Bhattacharya
Pacific Northwest National Laboratory
41 PUBLICATIONS **312** CITATIONS
SEE PROFILE

Sijie Lin
Tongji University
59 PUBLICATIONS **2,306** CITATIONS
SEE PROFILE

Physical Adsorption of Charged Plastic Nanoparticles Affects Algal Photosynthesis

Priyanka Bhattacharya,[†,‡] Sijie Lin,[†] James P. Turner,[†] and Pu Chun Ke*[,†,‡]

Laboratory of Single-Molecule Biophysics and Polymer Physics and Center for Optical Materials Science and Engineering Technologies, Clemson University, Clemson, South Carolina 29631

Received: June 14, 2010; Revised Manuscript Received: August 18, 2010

The physical adsorption of nanosized plastic beads onto a model cellulose film and two living algal species, *Chlorella* and *Scenedesmus*, has been studied. This adsorption has been found to ubiquitously favor positively charged over negatively charged plastic beads due to the electrostatic attraction between the beads and the cellulose constituent of the model and living systems. Such a charge preference is especially pronounced for *Chlorella* and *Scenedesmus*, whose binding with the plastic beads also depended upon algal morphology and motility, as characterized by the Freundlich coefficients. Using a CO_2 depletion assay, we show that the adsorption of plastic beads hindered algal photosynthesis, possibly through the physical blockage of light and air flow by the nanoparticles. Our ROS assay further indicated that plastic adsorption promoted algal ROS production. Such algal responses to plastic exposure may have implications on the sustainability of the aquatic food chain.

1. Introduction

For over a century, plastic has served our domestic and industrial needs, ranging from household utensils to cosmetics, sportswear, automobile parts, and oil and water pipelines. Plastic production, estimated at 260 million tons globally in 2007,[1] comes in various forms of natural materials (e.g., chewing gum, shellac), chemically modified natural materials (e.g., natural rubber, nitrocellulose), and completely synthetic materials (e.g., epoxy, polystyrene).

Due to its mass production, plastic rapidly accumulates in terrestrial and aquatic habitats and has become the most common type of marine litter worldwide.[2,3] Surveys of New Zealand beaches have revealed 100 000 plastic granules per meter of coastal zone.[4] Experimentally cleared beaches in Panama were seen to regain 50% of the original plastic burden after only 3 months.[5] Beaches in remote South Pacific Islands were collecting plastic debris and microplastic particles at levels comparable to industrialized areas.[6] The sources of plastic contamination of the marine environment include preproduction plastic pellets, powders, production scrap, consumer plastic debris, and microplastic particles used in industrial and domestic cleansers and in medical applications for drug delivery.[7−10] Plastic debris transported by wastewater and stormwater systems subsequently enters aquatic habitats where photo, chemical, and physical degradation processes fragment them into a wide array of particles sizes, ranging from macroscopic (>5 mm) to microscopic (<1 μm).[7]

Plastics such as polyvinylchloride, polystyrene, polycarbonate, polyethylene, polyester, and polyurethane have been shown to contain and release toxic monomers which have been linked to cancer and reproductive abnormities in humans, rodents, and invertebrates.[11] To date, it has been documented that plastic debris and macroplastic particles can pose a threat to marine fish, birds, turtles, and mammals through both direct and indirect ingestion, as well as physical entanglement in larger sized debris.[12] In addition, microplastic particles have been found to adsorb, concentrate, and transport hydrophobic contaminants from seawater into marine organism tissue. Low levels of polychlorinated biphenyls, dichlorodiphenyl, trichloroethane, and nonylphenol in seawater have been shown to be concentrated several orders of magnitude at the surfaces of plastic particles. In a recent study, phenanthrene contaminated polyethylene particles evolved into marine sediments, significantly enhancing the accumulation of this potentially toxic agent into the tissues of marine benthic organisms.[7]

In contrast to the global scale of plastic disposal, it remains poorly understood as to what extent discharged plastic may compromise environmental sustainability.[3,12−14] In this study, we first examine the physical adsorption of plastic nanoparticles on cellulose, a major structural component of the cell wall of green plants, many forms of algae, and the oomycetes. We then use both single-celled *Chlorella* and multicelled *Scenedesmus* to delineate the effect of algal morphology on plastic adsorption. To further assess algal photosynthetic activities, we measure the rate of CO_2 depletion resulting from the plastic adsorption. In order to evaluate algal responses to environmental stresses caused by the plastics, we monitor reactive oxygen species (ROS) production by the algal species. The use of plastic nanoparticles is a first in the field and is a logical extrapolation of microplastics continuously weathered by sunlight, rain, wind, and ocean waves, as well as decomposed by bacteria, microorganisms, and natural organic matter.[3] Furthermore, photooxidation functionalizes the surface of plastics to render them with different charge polarities, a basis for employing both positively and negatively charged plastics in this study. By using plastic nanoparticles, this study also contributes to the crucial assessment of engineered nanoparticles in the environment, a topic of tremendous importance for the safe development of nanotechnology and environmental protection.[15,16]

2. Materials and Methods

2.1. Characterization of Charged Polystyrene Nanospheres. Positively (Amidine Latex) and negatively (Carboxyl Latex) charged polystyrene (PS) beads were purchased from

* Corresponding author. E-mail: pcke11@clemson.edu. Phone: 8646560558. Fax: 8646560805.
[†] Laboratory of Single-Molecule Biophysics and Polymer Physics.
[‡] Center for Optical Materials Science and Engineering Technologies.

10.1021/jp1054759
Published on Web 09/13/2010

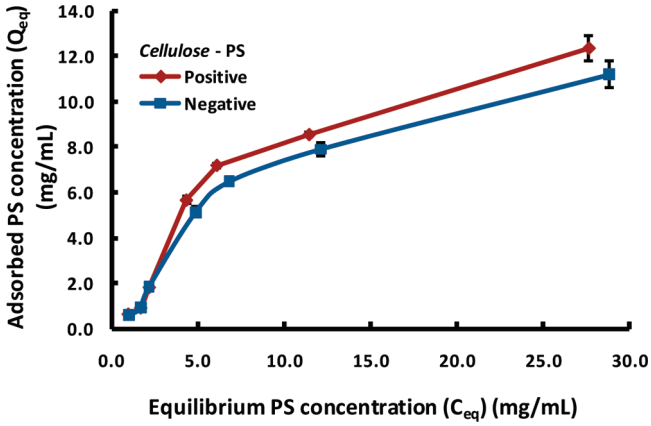

Figure 1. Adsorbed vs equilibrium PS bead concentration for cellulose thin films exposed to positively (maroon) and negatively (blue) charged PS beads.

Molecular Probes. The primary size and surface area of both types of beads were 20 nm and 2.5 × 10^6 cm^2/g, respectively. The amidine nanoparticles were stable at low pH and hence were dispersed in MES buffer with a pH of 6 at room temperature. The carboxyl nanoparticles were stable at neutral to high pH and were dispersed with Milli-Q water with a pH of 7.4 at room temperature. The PS nanoparticles existed as small agglomerates in both dispersions, and a complete breakdown by sonication was not performed, since this would not replicate a realistic representation of the natural conditions.

The surface charge of the as-supplied nanoparticles was characterized using a Zetasizer. Amidine PS beads showed an average zeta potential of 106 mV, and carboxyl PS beads had an average zeta potential of −40.4 mV. Both zeta potential measurements were performed for the PS beads of 4 mg/mL.

2.2. Interaction of PS Beads with Cellulose. Microcrystalline cellulose powder was purchased from Sigma-Aldrich and dissolved in LiCl/DMAc solvent according to the protocol given in ref 17. Cellulose surfaces are slightly anionic, due to the presence of carboxyl groups. Also, the surfaces of the cellulose microcrystallites possess sulfate groups, typically yielding an anionic charge on the order of 0.15e/nm^2.[18] Approximately 20 μL of the cellulose solution was added to each well of a standard plastic 96-well flat-bottomed plate and allowed to dry in a desiccator overnight. The solidified cellulose films were incubated with both positively and negatively charged PS beads of 1.6−40 mg/mL in their respective buffer solutions, for 24 h at room temperature. The plates were read at 340 nm using a microplate reader (Biotek Gen 5) to quantify the total concentrations of the nanoparticles. The measurements were repeated after washing away the nonadsorbed beads with their respective buffer solutions. On the basis of our measurements, an adsorption curve was plotted in Figure 1 for the amount of adsorbed PS beads (Q_{eq}) per milliliter of cellulose vs the equilibrium or unadsorbed amount of PS beads (C_{eq}). According to the Lambert−Beer law that the absorbance of a sample is proportional to its concentration, the amount of adsorbed PS beads was calculated by subtracting the absorbance read after wash from that before wash. The absorbance of the control cellulose was subtracted from both.

2.3. Interaction of PS Beads with Algae. Freshwater algae *Chlorella* and freshwater/saltwater *Scenedesmus* were purchased from Carolina Biological Supply Company. Chlorella is a genus of spherically shaped single-celled green algae, about 2−10 μm in diameter, and is without flagella, and *Scenedesmus* is a distinct genus of spherically to elliptically shaped, 2- to 32-celled green algae, 3−78 × 2−10 μm in dimensions, and possesses two pairs of flagella at each end. Both algal species contained cellulose in their cell walls and were grown in Alga-Gro freshwater medium.

The algal cells were incubated on a shaker separately with both positively and negatively charged PS beads of 0.08−0.8 mg/mL, for 2 h at room temperature. All dilutions were made in the algal growth media. Three samples of each concentration were prepared to ensure experimental repeatability and establish error bars.

2.4. Zeta Potential Measurements. A ZetaSizer (Nano ZS, Malvern Instruments) was used to measure the change in zeta potential of algae induced by the adsorption of the PS beads. The algal species were incubated with 4 mg/mL of positively and negatively charged PS beads on a shaker, for 24 h at room temperature (Figure 2).

2.5. Quantification of PS Bead Adsorption onto Algae. A UV−vis spectrophotometer (Biomate 3) was used to quantify the amount of the PS beads adsorbed on the algae. Absorbance was recorded at 260 nm before and after adding various concentrations of the PS beads to the algal growth medium. At this wavelength, the PS beads showed a strong absorbance. After 2 h of incubation, the algae−PS bead solution was filtered through membranes with a pore size of 0.2 μm (Whatman Anotop). A 2 μL portion of NaOH was added to the algae−PS solutions with anionic beads to facilitate their filtration through the weakly acidic membranes. At the low concentrations used, PS controls showed similar absorbances before and after filtration, indicating negligible mutual aggregation. Hence, all algal cells were blocked by the membranes due to their large size, while the absorbance of the filtrate indicated the amount of free or unadsorbed PS beads. The amount of adsorbed PS beads can be calculated by eq 1:

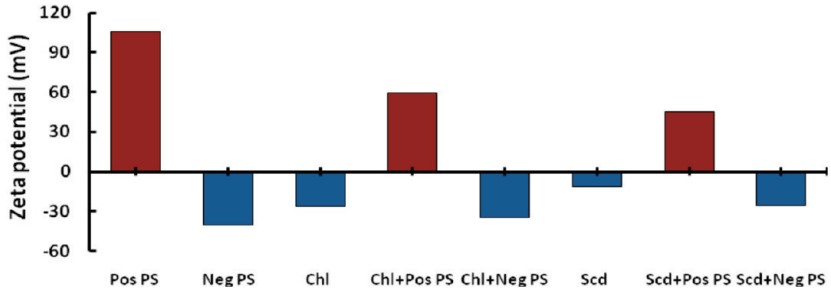

Figure 2. Zeta potentials of positively charged PS beads, negatively charged PS beads, *Chlorella* control, *Scenedesmus* control, and *Chlorella* and *Scenedesmus* mixed with positively and negatively charged PS beads. Abbreviations: "Pos" stands for positive, "Neg" for negative, "Chl" for *Chlorella*, and "Scd" for *Scenedesmus*.

$$\mathrm{Abs}_{\mathrm{absorbed}} = (\mathrm{Abs}_{\mathrm{PS+algae}} - \mathrm{Abs}_{\mathrm{algae}}) - \mathrm{Abs}_{\mathrm{filtered}} \quad (1)$$

where $\mathrm{Abs}_{\mathrm{filtered}}$ and $\mathrm{Abs}_{\mathrm{PS+algae}}$ denote the absorbance of the algae−PS bead solution after and before filtration, respectively, and $\mathrm{Abs}_{\mathrm{algae}}$ is the absorbance of the algae alone. An adsorption curve was established by varying the PS bead concentration from 0.08 to 0.8 mg/mL (Figure 3). Furthermore, the Freundlich model was used to fit the adsorption isotherms for PS beads. The Freundlich model, a modification of the Langmuir adsorption scheme,[19,20] appropriately describes rough, inhomogeneous adsorbent surfaces (i.e., algae) with multiple adsorption sites and also takes into account adsorbate−adsorbate (i.e., PS−PS) interactions:

$$Q_{\mathrm{eq}} = kC_{\mathrm{eq}}^{n} \quad (2)$$

where k is the coefficient indicating the affinity of PS beads for algae and n is a constant characteristic of the intensity of the adsorption. The parameters C_{eq} and Q_{eq} represent the concentrations of equilibrium or unadsorbed PS in the solution after filtration and the PS beads adsorbed on the algae at equilibrium, respectively.

2.6. Analysis of Algal Photosynthesis. The photosynthetic reaction is described by eq 3:

$$6CO_2 + 12H_2O + \mathrm{photons} = C_6H_{12}O_6 + 6O_2 + 6H_2O \quad (3)$$

To evaluate the effects of PS bead adsorption on algal bioactivities, the carbon dioxide depletion of the algae was examined in the presence of PS beads of 1.8−6.5 mg/L of algal solution. A bicarbonate indicator solution (0.2 g of thymol blue, 0.1 g of cresol red, in 0.01 M $NaHCO_3$) was prepared to monitor the depletion of CO_2, the activity of which is given by eq 4:

$$HCO_3^- + H^+ = H_2O + CO_2 \quad (4)$$

The algae−PS bead solution was mixed with the indicator solution, and the samples were tightly sealed to prevent gas exchange. During photosynthesis and respiration, the algae consumed or released CO_2 over time, causing the pH value of the indicator solution to increase or decrease, within a range of pH 4−8, accordingly. A transition from acidic to basic conditions was indicated by a color change from orange-red to deep purple, whereas a decrease in pH was indicated by a color change from orange-red to yellow, accompanied by an increase or decrease of absorbance at 574 nm, respectively. The changes in CO_2 depletion were then calculated on the basis of the increase or decrease of absorbance values for different sample concentrations (Figure 4). Absorbance of the control algal species and the control PS beads was also read over time.

2.7. ROS Measurements. An ROS assay, OxiSelect ROS Assay Kit (Cell Biolabs, Inc.), based on the fluorescent probe dichlorofluorescein (DCF) was used to scrutinize the generation of ROS in algal cells. DCF has been used previously in plant cell cultures to distinguish between sources of elicited ROS in tobacco epidermal cells[21] and visualize oxidative processes in response to mechanical stress.[22] In our experiment, specifically, 98 μL of algal cells were preincubated with 100 μL of a 20× diluted solution of DCFH−DA in algal growth media for 10 min in a black 96-well plate. Approximately 2 μL of the PS solutions was added to the plate to give a total bead concentration of 6.5 mg/L. The fluorescence of the mixtures was examined using a Cary Eclipse fluorescence spectrofluorometer (Varian Inc.) over time. The samples were excited at 480 nm and the emission read at 530 nm, with 20 nm excitation and emission slit widths and 10 s exposure time set for each well. To establish error bars, fluorometry experiments were performed in triplicates, and fluorescence intensities as a function of time were plotted (Figure 5).

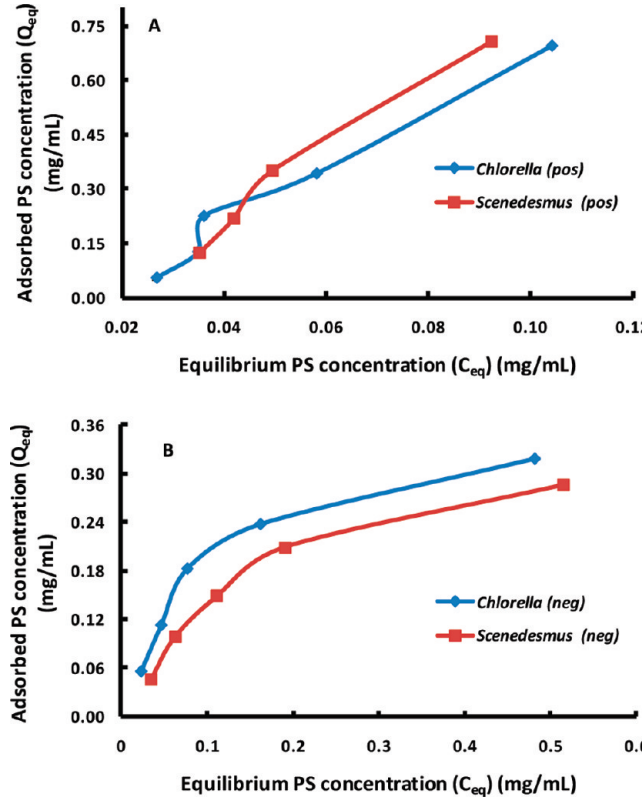

Figure 3. Adsorbed vs equilibrium PS concentrations for (A) positive and (B) negative PS beads exposed to *Chlorella* (blue) and *Scenedesmus* (maroon).

2.8. Scanning Electron Microscopy. The algal species were incubated with 4 mg/mL of differently charged PS beads for 24 h on a shaker. The mixtures were centrifuged at 30 000 rpm (27 090g RCF) for 3 min, and the supernatants were then removed. The pellets were resuspended in a 1:1 mixture of 2% osmium tetroxide and 4% sodium cacodylate buffer and kept overnight for fixation. The fixed algae−PS samples were then dehydrated in gradient concentrations of ethanol. Scanning electron microscopy (SEM) imaging was conducted using a Hitachi S4800 scanning electron microscope, operated at a 10 kV accelerating voltage (Figure 6).

3. Results and Discussion

3.1. Adsorption of PS Beads to Cellulose. Figure 1 shows the adsorption curves for both positively and negatively charged PS nanoparticles on a cellulose film. Under the set conditions, a significant increase of adsorption with PS bead concentration was observed for both types of beads. Saturation of adsorption was not reached for either of the charged beads, suggesting the possibility of a further increase of adsorption with increased PS bead concentration. The binding of both positively and negatively charged PS beads for the cellulose can be attributed to the hydrogen bond formation between the aromatic structures

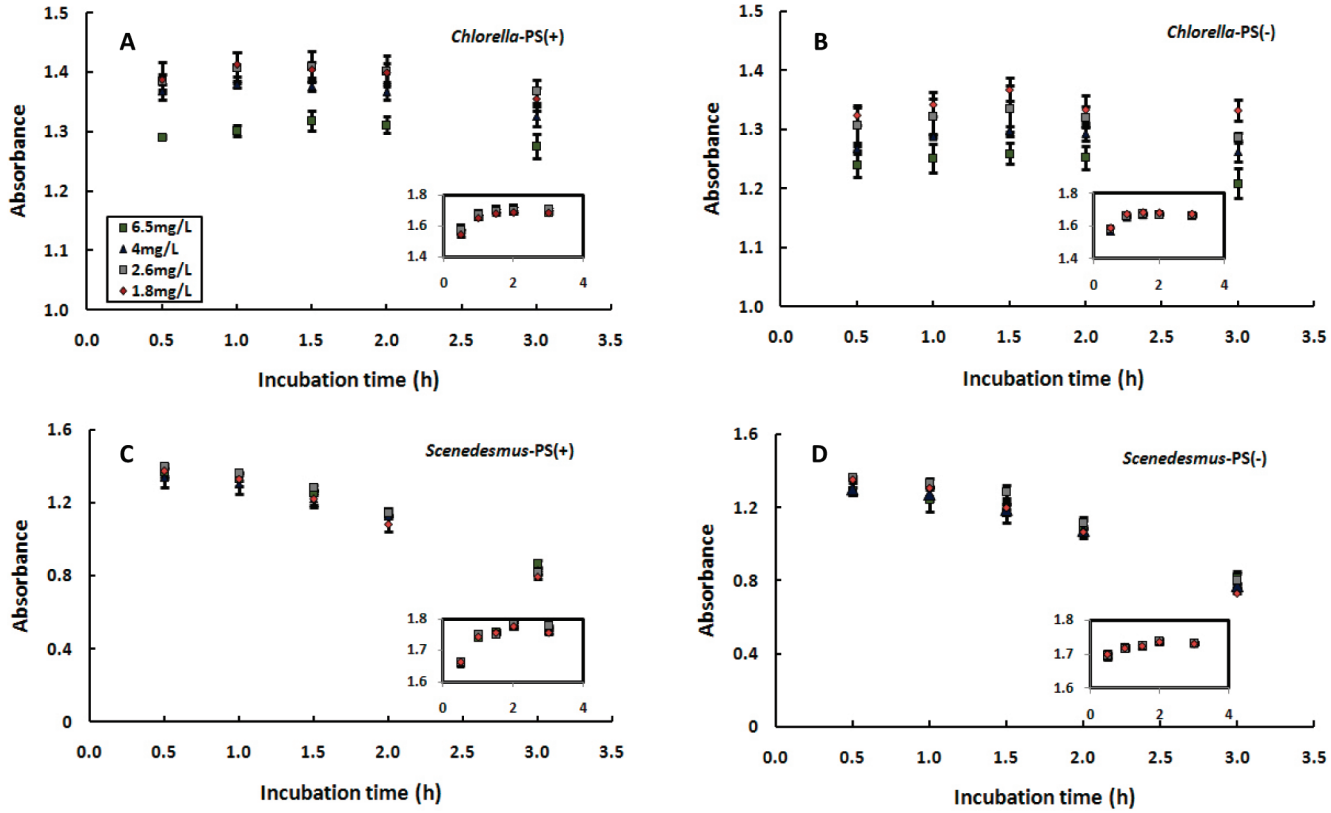

Figure 4. Absorbance vs incubation time for (A, B) *Chlorella* and (C, D) *Scenedesmus* exposed to positively and negatively charged PS beads of 1.8−6.5 mg/L of algal solution. The insets represent the sums of absorbance for the control algae and the four PS concentrations prior to their incubation. All absorbances read at 574 nm. The legend in the first plot applies to the symbols in all four plots and their insets.

of the cellulose and the PS beads. The roughness of the microcrystallite cellulose surfaces also provided numerous binding sites for the PS beads. Understandably, the negatively charged PS beads adsorbed slightly less than the positively charged beads, due to the electrostatic repulsion exerted by the carboxyl and sulfate groups in the cellulose.

3.2. Zeta Potential of PS Beads upon Algal Adsorption. Zeta potential measurements were performed to quantify the adsorption of charged PS beads to algal cells. As shown in Figure 2, *Chlorella* and *Scenedesmus* carried a zeta potential of −26.1 and −11.3 mV, respectively. Upon interaction with the positively charged PS beads, both algal species displayed an increase in zeta potential. Specifically, the zeta potential of *Chlorella*−PS beads increased by 85.8 mV, whereas the zeta potential of *Scenedesmus*−PS beads increased by 56.3 mV. In contrast, upon binding with the negatively charged PS beads, the zeta potential of *Chlorella*−PS beads slightly decreased by 9.0 mV, whereas the zeta potential of *Scenedesmus*−PS beads decreased by 14.6 mV. These measurements suggested that positively charged PS beads possessed a higher binding affinity than the negatively charged ones for the algae, consistent with our binding assay conducted with the PS beads and the cellulose film shown in Figure 1. Such consistency implied that cellulose played an essential role in initiating the binding between the algae and the plastics.

3.3. Adsorption of PS Beads to Algae. Figure 3A shows a rapid increase in adsorption with the dosage of positively charged PS beads, for both algal species. As expected, there was negligible adsorption observed for negatively charged PS beads (Figure 3B). To further characterize the adsorption processes, we fit our adsorption data to the Freundlich equilibrium model for the PS beads. The Freundlich coefficients were

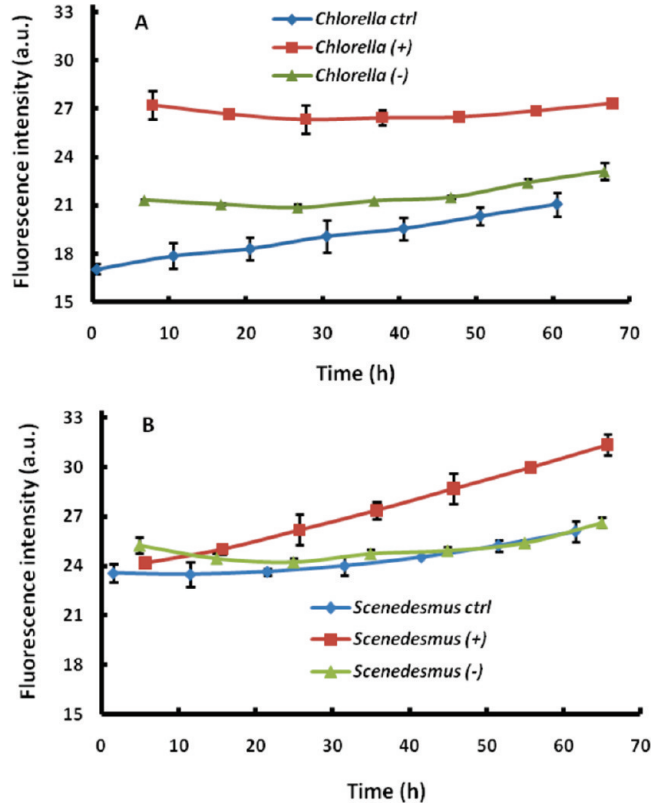

Figure 5. ROS production rates by (A) *Chlorella* (blue) and (B) *Scenedesmus* (blue) due to positive (maroon) and negative (green) PS adsorption. The fluorescence intensity is proportional to the level of the ROS produced. Concentrations of the positively and negatively charged PS beads: 6.5 mg/L of algal solution.

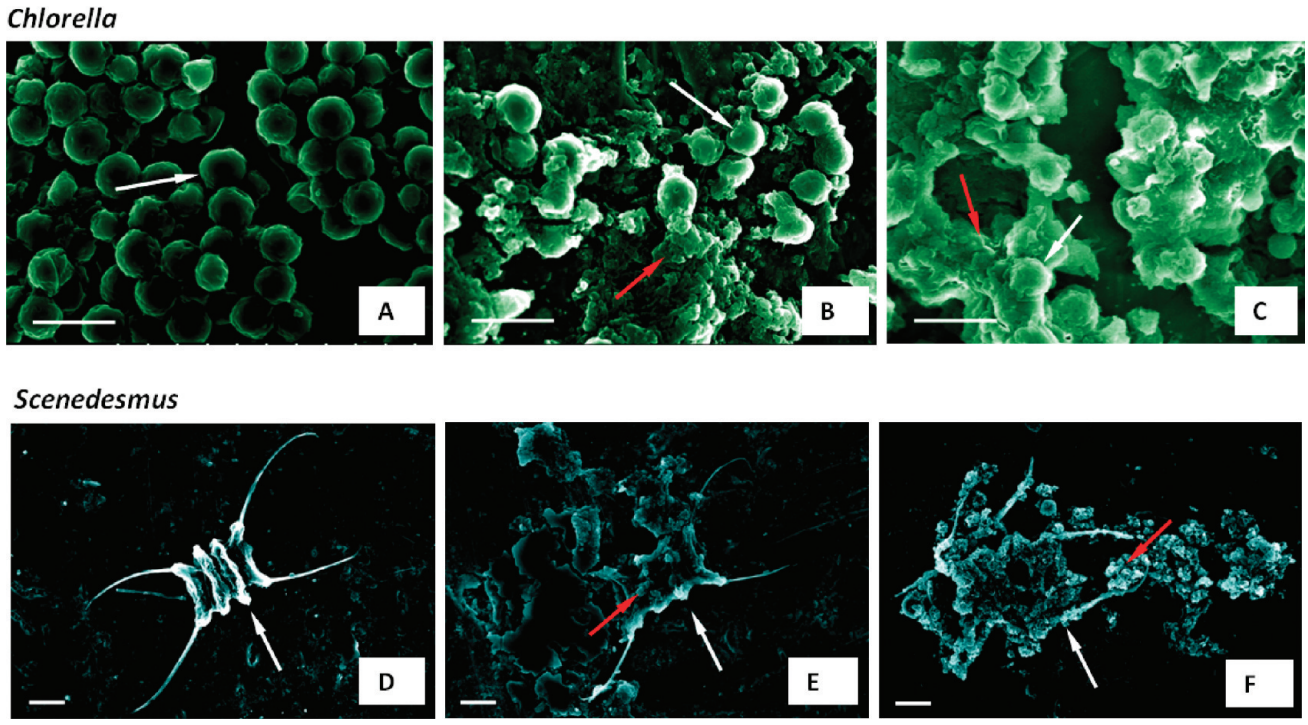

Figure 6. SEM images of algae adsorbed with PS beads. Incubation time: 24 h. (A) *Chlorella* control; (B) *Chlorella* with negatively charged PS beads; (C) *Chlorella* with positively charged PS beads; (D) *Scenedesmus* control; (E) *Scenedesmus* with negatively charged PS beads; (F) *Scenedesmus* with positively charged PS beads. Red arrows: nanoplastic aggregates. White arrows: algal cells. Scale bars for all: 5 μm.

obtained from the log−log plot of Q_{eq} vs C_{eq}. Here, the slope of the plot represents n, which indicates a deviation of the plot from linearity. The value k is inferred from the intercept of the plot. We obtained n values of 1.70 and 2.22 for *Chlorella* and *Scenedesmus* incubated with positively charged beads and 0.55 and 0.66 for negatively charged PS beads, respectively. As illustrated in Figure 3A, both the adsorption isotherms for *Chlorella* and *Scenedesmus* within the selected PS concentration range suggest a further increase in adsorption is possible with increased positively charged PS beads. Also, the affinity of negatively charged beads was higher for *Chlorella* than *Scenedesmus* (Figure 3B). This difference in the adsorption characteristics by the two algal species could be attributed to the more rugged morphology and higher total surface area of *Scenedesmus* than *Chlorella* (Figure 6). Specifically, *Chlorella* is spherical and single-celled, while *Scenedesmus* is an ellipsoidal, 4-celled assembly. In addition to morphology, *Scenedesmus*—unlike *Chlorella*—also possesses two pairs of flagella responsible for its agile motility in the aquatic environment. The k values obtained from the model fitting were 39.18 $(mg/mL)^{1-n}$ for *Chlorella* and 43.09 $(mg/mL)^{1-n}$ for Scenedesmus for the positively charged PS beads, further substantiating the observation that the algal species, especially Scenedesmus, possessed a high binding affinity for the positively charged PS beads. Although each *Scenedesmus* complex had more than twice the surface area than *Chlorella*, the total number of *Chlorella* cells outnumbered *Scenedesmus* by approximately 20 times per unit volume of the culture media. This led to a more pronounced adsorption and more robust nonspecific interaction between the *Chlorella* and the negatively charged PS beads, as indicated by Figure 3B. This was quantitatively substantiated by the Freundlich coefficient k, which was determined to be 0.58 and 0.54 $(mg/mL)^{1-n}$ for *Chlorella* and *Scenedesmus*, respectively.

3.4. Effect of PS Bead Adsorption on Algal Photosynthesis. Photosynthesis is a source for driving the metabolic processes of nearly all living species. Algae are positioned at the bottom of the food chain, and algal photosynthesis is a major source of much of earth's oxygen. Since algae consume CO_2 that is dissolved in the aquatic environment, the rate of CO_2 depletion serves as a key indicator for evaluating the photosynthetic activity of the organism. According to eq 4, an increase in pH corresponds to a decrease in the concentration of CO_2 in the bicarbonate indicator solution, which can be monitored by measuring the absorbance of the indicator at 574 nm.[23]

Figure 4 shows an addition of the absorbance of control algae and PS bead solutions prior to incubation. The absorbance of the indicator solution with control PS beads was stable over time at 574 nm for all concentrations, and that of the solution with control algae initially increased with time, gradually reaching stability, indicating an initial increasing rate of photosynthesis which became constant after 1.5 h. In contrast, as shown in Figure 4A and B, an increased dosage of PS beads added to *Chlorella* resulted in a significant decrease in CO_2 depletion at and above a PS concentration of 1.8 mg/L of algal solution. The trend is similar for both positively and negative charged PS beads. This hindered CO_2 depletion could be caused by the light shading effect of the adsorbed PS beads, and/or by obstructed CO_2 gas flow and nutrient uptake pathways.

In the case of *Scenedesmus*, adsorption of both positively and negatively charged PS beads also resulted in reduced absorbance with increased PS concentration, similar to that observed for *Chlorella*. Furthermore, the absorbance for *Scenedesmus* decreased approximately 40% over 4 h of incubation for all PS concentrations, indicating onset of algal respiration (Figure 4C and D). A decrease in absorbance of the indicator solution reflects a decrease in pH, corresponding to an increase in the CO_2 concentration in the algal solution. Such increased CO_2 concentration implies that the algae consumed the oxygen dissolved in the solution and released CO_2, a process known as cellular respiration. Cellular respiration in algae is a process by which food molecules are metabolized to convert to chemical energy for the cell. It occurs in the opposite direction as photo-

synthesis and is usually triggered in the absence of light. The energy produced by respiration is a source for algal motility. As shown in our SEM micrographs (Figure 6) and confocal imaging (data not shown), aggregation of the PS beads obstructed the flagella of the *Scenedesmus.* The algal species thus was forced to carry out respiration faster than photosynthesis in order to regain its motility. In addition, adsorption of the PS beads on algae could block light from reaching the photosynthesis centers and—although not observed in the present study—could damage the algal cell wall to induce pore formation, which could lead to uptake of the PS beads by the algae.

3.5. Effect of PS Adsorption on Algal ROS Production. In photosynthetic organisms, ROS are continuously produced as byproducts through various metabolic pathways localized in mitochondria, chloroplasts, and peroxisomes, and in response to environmental stresses such as pathogens, drought, light intensity, and contaminants.[24] In plants, ROS are mainly byproducts from the electron transport chains in chloroplasts. ROS are formed when electrons are diverted to O_2 but not CO_2 when photosynthetic efficiency decreases. Any reduction in electron transfer will hence enhance ROS production. The cell-permeable fluorogenic probe 2′,7′-dichlorodihydrofluorescin diacetate (DCFH-DA) is nonfluorescent and is deacetylated by cellular esterases to DCFH, which is rapidly oxidized to highly fluorescent DCF by ROS. The fluorescence intensity of the DCF is proportional to the ROS level within the cell cytosol. As can be seen in Figure 5A and B, for both algal species, adsorption of the positively charged PS beads resulted in a ROS burst and a higher rate of ROS production than the negatively charged beads. Also, *Scenedesmus* samples showed slightly higher levels of ROS production. These observations are consistent with our earlier results that plastic nanoparticles reduced photosynthesis for both algal species, and increased respiration in *Scenedesmus* led to increased O_2 activity (Figure 4).

Conclusions

In conclusion, adsorption of nanosized plastic beads has been found to hinder algal photosynthetic activities and promote their ROS production. Such adsorption depended on the physicochemical properties of the plastic and the morphological and biochemical properties of the algae. The plausible physical chemistry for the adsorption, much in favor of the positively charged plastic, includes electrostatic interaction, hydrogen bonding, and hydrophobic interaction between the algal species and the plastic. In view of our present findings, there is a need to further investigate plastics of different sizes and chemical compositions for assessing their adsorption with aquatic organisms and for acquiring a comprehensive understanding of aquatic responses to disposed plastic. One possible benefit of the hindered algal photosynthesis lies in the removal of toxic algal blooms from reservoirs that are used to storing drinking water, and from other aquatic ecosystems where overabundance of algae poses significant economical concerns.

Acknowledgment. This research was sponsored by an NSF CAREER Award # CBET-0744040 and a US EPA grant #R834092. P.B. acknowledges the support of a COMSET graduate fellowship.

References and Notes

(1) Plastics-Europe. Analysis of plastics production demand and recovery in Europe for 2008. Association of Plastics Manufacturers (2008).
(2) Derraik, J. G. B. *Mar. Pollut. Bull.* **2002**, *44*, 842.
(3) Thompson, R. C.; Olsen, Y.; Mitchell, R. P.; Davis, A.; Rowland, S. J.; John, A. W. G.; McGonigle, D.; Russell, A. E. *Science* **2004**, *304*, 838.
(4) Gregory, M. R.; Kirk, R. M.; Mabin, M. C. G. *N. Z. Antarct. Rec.* **1984**, *6*, 12.
(5) Garrity, S. D.; Levings, S. C. *Mar. Pollut. Bull.* **1993**, *26*, 317.
(6) Benton, T. G. *Biol. J. Linn. Soc.* **1995**, *56*, 415.
(7) Teuten, E. L.; Rowland, S. J.; Galloway, T. S.; Thompson, R. C. *Environ. Sci. Technol.* **2007**, *41*, 7759.
(8) Gregory, M. R. *Mar. Pollut. Bull.* **1996**, *32*, 867.
(9) Ye, S.; Andrady, A. L. *Mar. Pollut. Bull.* **1991**, *22*, 608.
(10) Silverman, J. http://science.howstuffworks.com/great-pacific-garbage-patch.htm (accessed Sept 19, 2007).
(11) Vom Saal, F. S.; Hughes, C. *Environ. Health Perspect.* **2005**, *113*, 926.
(12) Ward, J.; Shumway, S. *J. Exp. Mar. Biol. Ecol.* **2004**, *300*, 83.
(13) Kanai, M.; Murata, Y.; Mabuchi, Y.; Kawahashi, N.; Tanaka, M.; Ogawa, T.; Doi, M.; Soji, T.; Herbert, D. C. *Anat. Rec.* **1996**, *244*, 175.
(14) Olivier, V.; Rivière, C.; Hindié, M.; Duval, J.-L.; Bomila-Koradjim, G.; Nagel, M.-D. *Colloids Surf., B* **2004**, *33*, 23.
(15) Wang, X. L.; Lu, J. L.; Xing, B. *Environ. Sci. Technol.* **2008**, *42*, 3207.
(16) Mauter, M. S.; Elimelech, M. *Environ. Sci. Technol.* **2008**, *42*, 5843.
(17) McCormick, C. L.; Callais, P. A.; Hutchinson, B. H. *Macromolecules* **1985**, *18*, 2394.
(18) Dong, X. M.; Kimura, T.; Revol, J.-F.; Gray, D. G. *Langmuir* **1996**, *12*, 2076.
(19) Awan, M. A.; Dimonie, V. L.; Filippov, L. K.; El-Aasser, M. S. *Langmuir* **1997**, *13*, 130.
(20) Prescott, S. W.; Fellows, C. M.; Considine, R. F.; Drummond, C. J.; Gilbert, R. G. *Polymer* **2002**, *43*, 3191.
(21) Allan, A. C.; Fluhr, R. *Plant Cell* **1997**, *9*, 1559.
(22) Yahraus, T.; Chandra, S.; Legendre, L.; Low, P. S. *Plant Physiol.* , *109*, 1259.
(23) Lin, S.; Bhattacharya, P.; Brune, D. E.; Rajapakse, N.; Ke, P. C. *J. Phys. Chem. C* **2009**, *113*, 10962.
(24) Liu, W.; Au, D. W. T.; Anderson, D. M.; Lam, P. K. S.; Wu, R. S. S. *J. Exp. Mar. Biol. Ecol.* **2007**, *346*, 76.

JP1054759